

MRS Advances © 2018 Materials Research Society DOI: 10.1557/adv.2018.305

A Combined Experimental and Theoretical Study of Lithiation Mechanism in ZnFe₂O₄ Anode Materials

 $\label{eq:Lei Wang} Lei \ Wang^{1,t}, \ Alison \ McCarthy^{2,t}, \ Kenneth \ J. \ Takeuchi^{1,2,}, \ Esther \ S. \ Takeuchi^{1,2,3}, \ and \ Amy \ C. \ Marschilok^{1,2,3,*}$

¹Department of Chemistry, Stony Brook University, Stony Brook, NY 11794

²Department of Materials Science and Chemical Engineering, Stony Brook University, Stony Brook, NY 11794

³Energy and Photon Sciences Directorate, Brookhaven National Laboratory, Upton, NY 11973

 ${}^t\!Equivalent\ contributions.\ \ {}^*corresponding\ author:\ amy.marschilok@stonybrook.edu.$

ABSTRACT

 $ZnFe_2O_4$ (ZFO) represents a promising anode material for lithium ion batteries, but there is still a lack of deep understanding of the fundamental reduction mechanism associated with this material. In this paper, the complete visualization of reduction/oxidation products irrespective of their crystallinity was achieved experimentally through a compilation of in situ X-ray diffraction, synchrotron based powder diffraction, and ex-situ X-ray absorption fine structure data. Complementary theoretical modelling study further shed light upon the fundamental understanding of the lithiation mechanism, especially at the early stage from $ZnFe_2O_4$ up to $Li_xZnFe_2O_4$ (x = 2).

INTRODUCTION

 $ZnFe_2O_4$ (ZFO) possesses an ordered spinel structure, with close-packed O^{2-} as well as Zn^{2+} and Fe^{3+} preferentially occupying the tetrahedral (8a) and octahedral (16d) sites, respectively. The low toxicity, facile synthesis method, structural stability associated with spinel structure, along with its high theoretical capacity (1000 mA h g⁻¹) have rendered ZFO as a promising anode material. [1]

With respect to the reduction mechanism, it is widely believed that the Li⁺ ions first insert into the 16c vacancies in the spinel structure (eq. 1), where x is reported within the range of 0.2-2. Subsequently, the discharge process proceeds to form metallic species, during which the intermediates are yet unidentified (eq. 2), which contributes to 890 mAh/g capacity. The Zn⁰ has been reported to form the Zn-Li alloy (eq.3), which accounts for one electron equivalent from discharge current and leads to another 110 mAh/g capacity.

$$ZnFe_2O_4 + xLi^+ + xe^- \rightarrow Li_xZnFe_2O_4$$
 (1)
 $Li_xZnFe_2O_4 + (8-x)Li^+ + (8-x)e^- \rightarrow Zn^0 + 2Fe^0 + 4Li_2O$ (2)
 $Li^+ + e^- + Zn \rightarrow ZnLi$ (3)

It is worth noting that the alloy reduction mechanism was only noted in two reports[2, 3] in ex-situ electrodes reduced below 0.01 V. For the oxidation products, it is still controversial whether FeO[4] or $Fe_2O_3[5]$ is formed along with ZnO as the final products.

Herein, our study focuses on (i) identifying whether alloy formation can be observed under more typical discharge conditions and whether it can account for the high delivered capacity; (ii) confirming the formation of FeO or Fe₂O₃ during the recharging process; as well as (iii) understanding the structural evolution during the early lithiation stage.

EXPERIMENTAL

ZFO nanoparticles were prepared using a precipitation method followed by hydrothermal reaction at 220°C for 12 h.[1] Electrodes were prepared using a slurry cast method with ZFO as active material combined with carbon and polyvinylidene fluoride binder at a mass com position of 70:20:10. Cyclic voltammetry (CV) data were collected between 0.2 and 3.0 V at a scan rate of 0.1 mV/s. Undischarged material, material reduced to 0.5ee, 2ee, 4ee, 8ee, 12ee (fully reduced), and oxidized ZFO coatings were measured using x-ray absorption spectroscopy (XAS) at Argonne National Laboratory. X-ray powder diffraction (XPD) of undischarged, 1ee, and fully discharged samples were taken at National Synchrotron Light Source-II (NSLS-II) at Brookhaven National Laboratory. Atomic pair distribution function measurements (PDF) were taken of undischarged and fully discharged ZFO pellets. For the theoretical calculations, density functional theory (DFT) implemented in the Vienna ab initio simulation package (VASP) was employed,[6] using the PAW potential[7] and GGA-PBE exchange-correlation functional[8] and a kinetic energy cutoff of 520 eV. The DFT calculations described a sequence for the Li⁺ ions to intercalate into the ZFO bulk system, where all possible sites for each inserted Li⁺ ion were considered.

RESULTS AND DISCUSSION

Electrochemical testing and in-situ XRD

Comparing the CV measurements (Figure 1A) with the galvanostatic tests (Figure 1B), the first reduction can be attributed to insertion and phase change, with a phase change on oxidation. The three peaks in the first cycle of the CV correspond to the three labelled plateaus from the galvanostatic profile. The two small cathodic peaks at ~ 1.46 V (peak a) and ~ 1.04 V (peak b), followed by a major sharp peak at ~ 0.73 V (peak c) can be assigned to a first reduction process occurring with Li⁺ insertion to 16c site, accompanied by the migration of Zn²⁺ from 8a to 16c site, followed by the formation of Fe metal concurrent with an amorphous ZnO phase, which agrees well with the following XAS and DFT results. Subsequent reductions that occur after the initial result in less phase changes. *In-situ* XRD data was taken at each 0.5 electron equivalent over

the first 7.5 electron equivalents (ee) (Figure 1C), where the ZFO (044) peak located at 62 degrees was chosen to probe the phase change during the lithiation process. Drastic peak shift to a lower angle was noticed between scans 3 and 4 (Figure 1D), corresponding to 1.0 and 1.5ee discharge. Further lithiation after scan 9 (4ee discharge) led to a decrease in intensity (Figure 1E), indicating a material amorphization process. To better observe the change of crystallinity, the intensity as well as full width at half maximum (FWHM) associated with the (044) peak as a function of scan numbers were displayed in Figure 1F. Our data clearly suggested that during lithiation, the intensity of the peak (044) continues to decrease. Specifically, the intensity after scan 9 (4ee discharge) is dramatically (80%) lower than that in scan 6. After full discharge (scan 16), a drastic increase in the FWHM is noted, which further confirms the amorphization of the materials.[9]

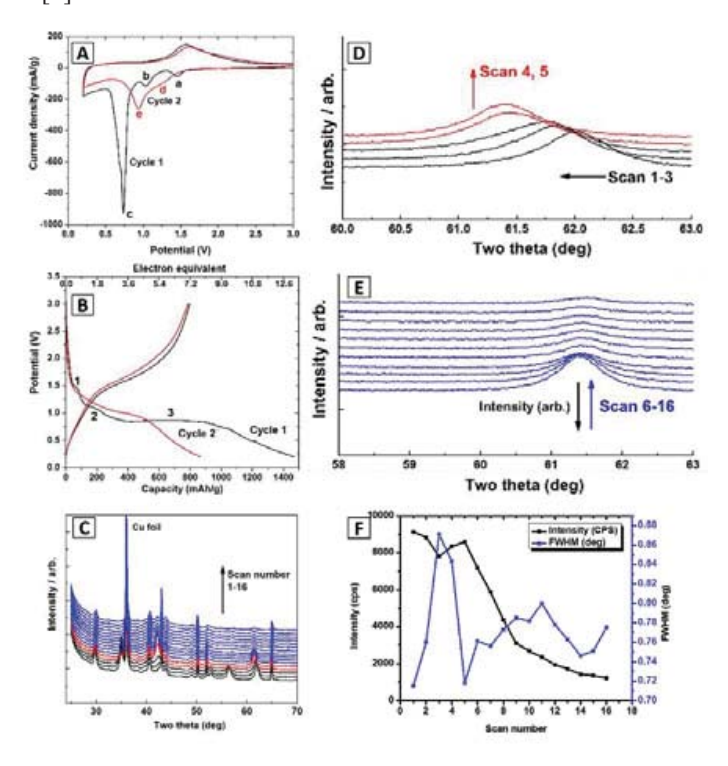


Figure 1. (A) Cyclic voltammogram of ZFO electrode at 0.1 mV/s for cycle 1 and 2; (B) galvanostatic profile for cycle 1 and 2 of ZFO electrode at 100 mA/g current density; (C) in situ XRD stack plot during galvanostatic reduction; (D) (044) peak evolution of the first five scans; (E) (044) peak evolution from scan 6 to 16; and (F) intensity as well as width of the (004) peak as a function of scan number. Figure is reprinted with permission from ref. 6, copyright 2017, of American Chemical Society.

Synchrotron XPD results and PDF analysis

Synchrotron based XPD was performed to investigate the structure of the 1ee reduced sample $LiZnFe_2O_4$ in detail through Rietveld refinement (Figure 2A). The refinement showed that there was a 0.56% expansion when compared to the starting lattice parameter and 46% of the Zn migrated from the 8a site to the 16c site, while the rest of the Zn remained in the 8a site, which was confirmed by the DFT prediction of a

50:50 split between the sites. Subsequently, PDF spectra of the undischarged and fully discharged ZFO pellets were compared (Figure 2B). The undischarged ZFO matched well with the crystal structure determined from Rietveld refinement. After lithiation to 0.2V, the sharp peak around 2.5 Å was ascribed to bcc Fe metal with an approximate crystallite size of 1.8 nm. The fitted data also suggested that 15% of the active material was not fully reduced even with a slow discharge rate of C/200. No distinct peaks were noticed from the ZnO species, which suggested that the phase was highly disordered and small.

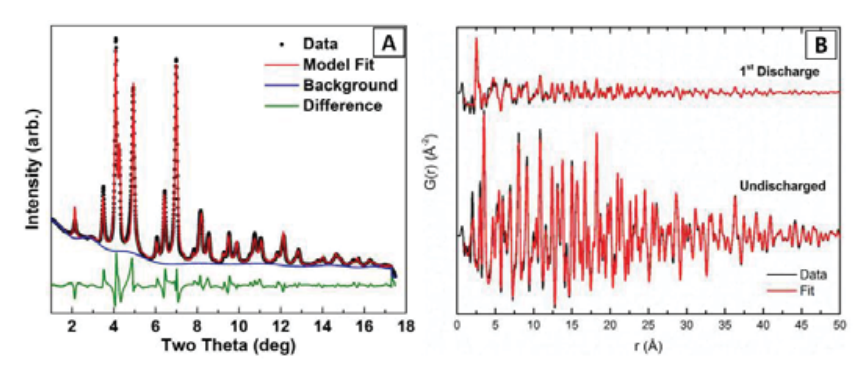


Figure 2. (A) Rietveld analysis on 1ee discharged ZFO; (B) PDF spectra of undischarged and fully discharged ZFO pellets (black) with corresponding fitted structure results (red).

X-ray absorption spectroscopy (XANES and EXAFS)

X-ray absorption near edge spectroscopy (XANES) of both Fe and Zn K-edges of *ex-situ* electrodes at various discharge levels (Figure 3A) was measured to track the changes in their oxidation states. The Fe K-edge energy shifted slightly from 7126 eV in the undischarged state to 7124 eV at 0.5, 2, and 4ee. A metallic-like edge position of 7112 eV, corresponding to the Fe metal standard, was observed when the material was discharged to 8ee and remained in the same position as the electrode was reduced to 0.2V. Zn K-edge energy only shifted from 9664 eV in the undischarged state to 9663 eV at 4ee. Upon reduction to 0.2 V, the edge shifted to 9662 eV, which was much higher than that of the metallic Zn (9659 eV), indicating that Zn metal or ZnLi alloy had not yet formed at this state. In fact, most of the Zn atoms were still in their oxidized state.

The extended X-ray absorption fine structure (EXAFS) region of the XAS spectra was subsequently analyzed as R-space plots (Fourier transforms of $k^2|\chi(R)|$), Figure 3B. By measuring the distances of the neighboring Fe and Zn atoms, structural evolution information was provided complimentary to the oxidation state information provided by the XANES analysis. Various bond distances at different discharge levels suggested that Zn^{2+} ions began to migrate at 0.5ee discharge from 8a to 16c sites, evolving into a new phase of $[Zn]_{16c}[Fe_2]_{16d}O_4$ by 2ee. Fe metals and amorphous ZnO were formed at 8ee discharge, which remained similar until reduction to 0.2 V.

After the first oxidation, the Fe K-edge of the ZFO electrode was further analyzed using both XANES (Figure 3C) and EXAFS (Figure 3D). Our data suggested that the oxidized electrode demonstrated some reversibility, but the Fe was not fully oxidized to 3⁺. However, upon the first charge, no observation of the Fe metal-like distance (~2.50 Å) was noted, indicating high reversibility of the iron species between Fe metal on discharge and highly disordered FeO on charge at these early cycles.

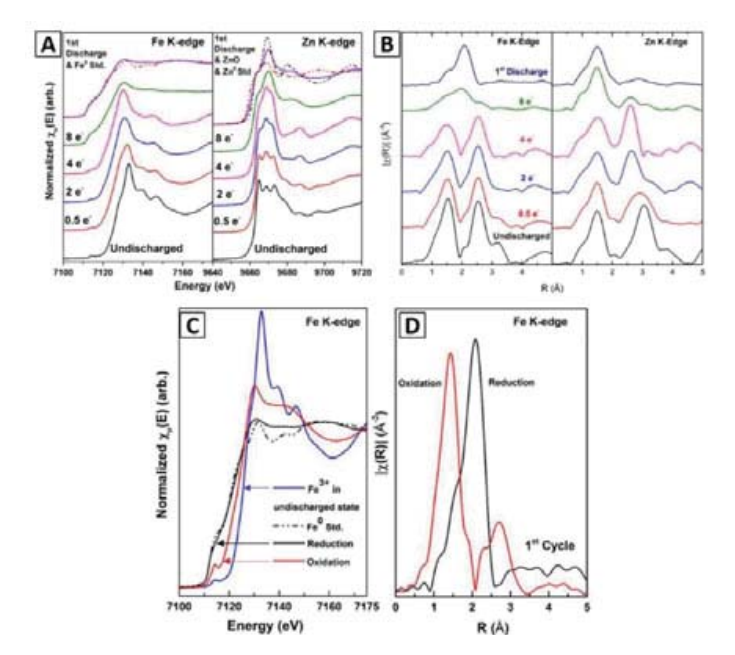


Figure 3. (A-B) XANES and EXFAS of the Fe and Zn K-edges at different discharge levels. (C-D) Comparison of Fe K-edge at first discharge (black) and recharge back to 3.0 V (red).

Density functional study (DFT) of initial discharge process to Li_xZnFe₂O₄ (x= 2)

To provide in-depth understanding of the mechanism associated with the early lithiation stage, DFT was used to probe the preferred structures of $ZnFe_2O_4$ up to $Li_xZnFe_2O_4$ (x=2).[1] The calculation indicated that $Li_xZnFe_2O_4$ at the initial discharging (x<0.5) was not stable. With x increasing to 1, the Li^+ preferably intercalated into octahedral 16c sites, which was accompanied by Zn^{2+} ion migration from tetrahedral 8a sites to 16c sites starting at x = 0.25. The most stable $Li_xZnFe_2O_4$ occurred when x=1, where Li^+ and Zn^{2+} ions filled all the available 16c sites (Figure 4A). The stability decreased for $1 < x \le 2$ due to the occupation of Li^+ ions in the less active tetrahedral 8a/48f/8b sites. It is worth noting that open-circuit-voltages (OCVs) estimated based on the stable intermediate structures from the DFT calculations were in good agreement with the experimental values (Figure 4B).

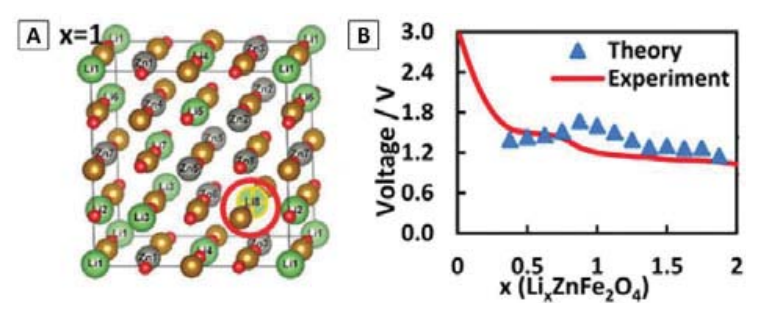


Figure 4. (A) DFT optimized structures of $\text{Li}_x \text{ZnFe}_2 \text{O}_4$ with x=1 (green: Li; gray: Zn; yellow: Fe; red: O), where all the octahedral sites are occupied by either Li^+ or Zn^{2^+} . (B) Comparison of DFT-estimated OCV (symbols) for Li^+ ion intercalation into ZFO with the experimental values (lines).

CONCLUSIONS

In the current work, a combined experimental and theoretical study was presented to provide in-depth understanding of the fundamental discharge/charge mechanisms associated with ZFO electrodes. Our data suggest that at the early discharge stage (0 < x \leq 2), Li⁺ ions preferably intercalate into the octahedral 16c sites over the tetrahedral 8a/48f/8b sites, which is always accompanied by the migration of nearby Zn²⁺ from the 8a to the 16c site starting from x=0.25 and ending at x between 0.875 and 1.125. After full reduction to 0.2 V, Fe metal and an amorphous ZnO phase are formed, with no evidence of Zn metal or ZnLi alloy formation. The recharged electrode was found to contain both ZnO and FeO, instead of Fe₂O₃.

The future direction of ZFO anodes will be focused on developing other advanced characterization techniques to monitor the electrochemical processes in situ, as well as strategies to optimize the performance of the ZFO electrode, through physical and chemical manipulation of crystallite size, morphology, and electrode architectures.

ACKNOWLEDGEMENTS

The authors acknowledge the Center for Mesoscale Transport Properties, an Energy Frontier Research Center supported by the U.S. Department of Energy, Office of Science, Basic Energy Sciences, under award #DE-SC0012673 for financial support. MRCAT operations are supported by the Department of Energy and the MRCAT member institutions. This research used resources of the Advanced Photon Source, a U.S. Department of Energy (DOE) Office of Science User Facility operated for the DOE Office of Science by Argonne National Laboratory under Contract No. DE-AC0206CH11357. Use of the National Synchrotron Light Source II, Brookhaven National Laboratory, was supported by the U.S. Department of Energy, Office of Science, Office of Basic Energy Sciences, under Contract No. DE-SC0012704. The DFT calculations were performed using computational resources at the Center for Functional Nanomaterials at Brookhaven National Laboratory, an Office of Science User Facility under Contract No. DE-SC0012704.

REFERENCES:

- 1. H. Guo, Y. Zhang, A. C. Marschilok, K. J. Takeuchi, E. S. Takeuchi and P. Liu, Phys. Chem. Chem. Phys. 19 (38), 26322-26329 (2017).
- Y. N. NuLi, Y. Q. Chu and Q. Z. Qin, J. Electrochem. Soc. 151 (7), A1077-A1083 (2004).
- 3. X. W. Guo, X. Lu, X. P. Fang, Y. Mao, Z. X. Wang, L. Q. Chen, X. X. Xu, H. Yang and Y. N. Liu, Electrochem. Commun. **12** (6), 847-850 (2010).
- 4. Y. Sharma, N. Sharma, G. V. S. Rao and B. V. R. Chowdari, Electrochim. Acta **53** (5), 2380-2385 (2008).
- 5. Z. Xing, Z. C. Ju, J. Yang, H. Y. Xu and Y. T. Qian, Nano Res. 5 (7), 477-485 (2012).
- 6. G. Kresse and J. Furthmuller, Comput. Mater. Sci. 6 (1), 15-50 (1996).
- 7. P. E. Blochl, Phys. Rev. B **50** (24), 17953-17979 (1994).
- 8. J. P. Perdew, K. Burke and M. Ernzerhof, Phys. Rev. Lett. 77 (18), 3865-3868 (1996).
- 9. Y. Zhang, C. J. Pelliccione, A. B. Brady, H. Guo, P. F. Smith, P. Liu, A. C. Marschilok, K. J. Takeuchi and E. S. Takeuchi, Chem. Mater. **29** (10), 4282-4292 (2017).